Acta Ciencia Indica, Vol. XL P, No. 2, 49 (2014)

ELECTRONIC PROPERTIES OF BORON AND NITROGEN DOPED GRAPHENE

S. CHANDRA

Department of Physics, Panjab University, Chandigarh – 160014, India

RECEIVED : 25 April, 2014

Graphene can be doped with boron and nitrogen, B_2H_6 has been generally used as the boron source while NH_3 or pyridine is employed as the nitrogen source. Graphene with boron and nitrogen brings about significant change in the electronic structure and properties. Such doping not only results in desirable properties but also allows manipulation of properties for specific purposes. Doping with boron and nitrogen causes marked changes in the Raman spectra. In this paper we present the synthesis and characterization of boron and nitrogen doped graphene.

KEYWORDS : Raman spectroscopy, Transmission electron microscopy, Chemical Vapor Deposition, Few layer graphenes, Raman scattering, Electronic properties.

INTRODUCTION

Graphene has emerged as an exciting material today because of the novel properties associated with its two dimensional structure [1-2]. Single layer graphene is a one atom thick sheet of carbon atoms densely packed into a two dimensional honeycomb lattice. It is the mother of all graphitic forms of carbon including zero-dimentional fullerences and one-dimentional carbon nanotubes [2-3]. The remarkable feature of graphene is that is a Dirac solid, with the electron energy being linearly dependent on the wave vector near the vertices of the hexagonal Brillouin zone. It exhibits room-temperature fractional quantum Hall effect [4] and ambipolar electric field effect along with ballistic conduction of charge carriers [5]. It has been reported recently that a top-gated single layer graphene transistor is able to reach electron or hole doping levels of upto 5×10^{13} cm^{-2}.

The doping effects are ideally monitored by Raman Spectroscopy. Thus, the *G* band in the Raman spectrum stiffens for both electron and hole doping and the ratio of the intensities of the 2D and G band varies sensitively with doping. Molecular charge transfer induced by electron donor and acceptor molecules also give rise to significant changes in the electronic structure of few-layer graphenes, as evidenced by changes in the Raman spectrum [6-8]. Charge-transfer by donor and acceptor molecules soften and stiffen the G band respectively. The difference between electrochemical doping and doping through molecular charge transfer is noteworthy. It is of fundamental interest to investigate how these effects compare with the effects of doping graphene by substitution with boron and nitrogen and to understand dopant induced perturbations on the properties of graphene. We have carried out first principles DFT calculations to understand the effect of substitutional doping on the structure of graphene and its electronic properties.

EXPERIMENTAL METHOD

To prepare B and N doped graphenes, we have exploited our recent findings that are discharge between carbon electrodes in a hydrogen atmosphere yields graphenes (HG) with two to three layers. One set of boron graphene samples (BG1) was prepared by carrying our arc discharge of graphite electrodes in the presence of hydrogen, helium and diborane (B_5H_6). B_2H_6 vapor was carried to the are chamber by passing hydrogen (200 torr) through B_2H_6 generator and subsequently by passing He (500 torr). Second set of boron doped samples (BG2) was prepared by carrying out arc discharge using a boron stuffed graphite electrode (3 at % boron) in the presence of H_2 (200 torr) and He (500 Torr).

One set of nitrogen doped graphene samples (NG1) was prepared by carrying out arc discharge of graphite electrodes in the present H_2, He and pyridine vapors. Pyridine vapour was carried to the are chamber by passing hydrogen (200 torr) through pyridine bubbler and subsequently by passing He (500 torr). Second set of nitrogen doped samples (NG2) was prepared by carrying out arc discharge of graphite electrodes in the presence of H_2 (200 torr), He (200 torr) and NH3 (300 torr). Transformation of nanodiamond was also carried out in the presence of He and Pyridine vapour at 1650ºC to obtain N doped graphene (NG3). We have also carried out the transformation of nanodiamond in the presence of pyridine (NG3) to obtain N doped graphene. All the doped samples were characterized by variety of physical methods.

RESULTS AND DISCUSSION

3.1. Electronic properties

X-ray photoelectron spectroscopic (XPS) analysis shows that the BG1 and BG2 contained 1.2 and 3.1 at % of boron respectively, while the electron energy loss spectroscopy (EELS) data show the content of boron in these samples to be 1.0 and 2.4 at % respectively. In Fig. 1.

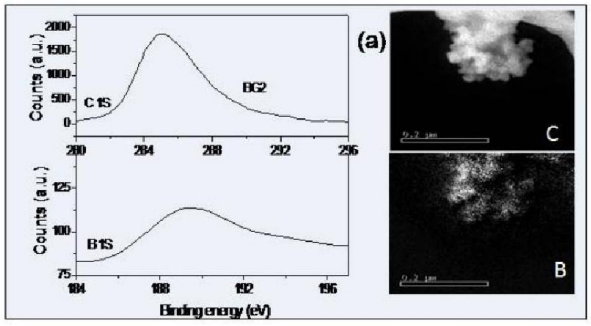

Fig. 1 - (a) C 1s and B 1s XPS signals and B-doped graphene (BG2), EELS elemental mapping of C and B of BG2.

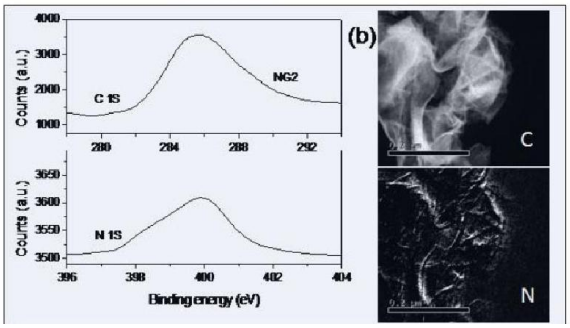

Fig. 2 - (b) C 1s and N 1s XPS signals of N-doped graphene (NG2), EELS elemental mapping of C and N of NG2.

We show typical core level XPS data of BG2 along with the elemental mapping by EELS. XPS data show NG1, NG2 and NG3 to contain 0.6, 0.9 and 1.4 at % of nitrogen respectively. In Fig. 2, we show XPS data of the NG2 sample along with EELS elemental mapping. The asymmetric shape of the N1s peak indicates the existence of at least two components. On deconvolution, we find peaks at 398.3 eV and 400 eV, the first one being characteristic of pyridinic nitrogen and the second of nitrogen in the graphene sheets [13-14]. Analysis of the (002) reflections in the X-ray diffraction (XRD) patterns shows that the B and N doped samples contained 2-3 layers on an average. This is also confirmed by the TEM images Fig. 3. Atomic force microscopy images also showed the presence of 2-3 layers in the BG and NG samples, with occasional presence of single layers. TGA shows that the B and N doped undergo combustion at a slightly lower temperature than the parent graphene (580ºC).

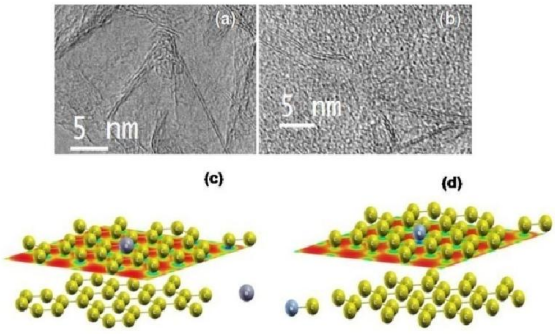

Fig. 3 – TEM images of (a) B-doped graphene (BG2), (b) N-doped graphene (NG1) STEM images of (c) B- and (d) N-doped bilayers.

We examined the Raman Spectra of all the BG and NG samples in comparison with the spectrum of the pure graphene sample (HG), prepared by the H_2-discharge method Fig. 4. The Raman spectrum [with 632.8 nm excitation] of these samples shows three main features in 1000-3000 cm^{-1} region, the G band (~ 1570 cm^{-1}), the defect – related D band [14] (~ 1320 cm^{-1}), and the 2D band (~ 2640cm^{-1}). It is noteworthy that the G band stiffens both with boron and nitrogen doping. This is similar to what happens with electrochemical doping [6]. The shift in the case of BG2, with a higher B-content, is larger than with BG1. In the case of N-doped graphene, NG3, with the highest N content, shows the largest shift. The intensity of the D band is higher with respect to that of the G band in all the doped samples. On doping, the relative intensity of the 2D band generally decreases with respect to the G band. We calculate in plane crystallite sizes (L_a) of the undoped as well as doped graphene samples by following formula [15].

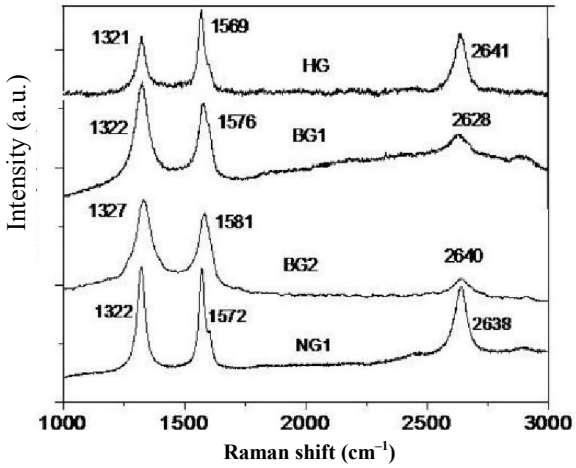

Fig. 4 - Raman spectra of undoped (HG) and doped (BG and NG) graphene samples.

$$\text{La(nm)} = (2.4 \times 10^{-10})\ \lambda^4 \left(\boldsymbol{I_D} / \boldsymbol{I_G} \right)^{-1} \quad \ldots (1)$$

Here λ is wavelength used for Raman measurements and I_D, I_G respectively intensity of *D* and *G* band. The crystalline size of the HG, BG1, BG2, NG1, NG2 and NG3 samples are respectively 64, 30, 26, 43, 41 and 10 nm. Doped graphene samples show low in crystallite sizes compared to undoped graphene samples. We also find that the BG and NG samples exhibit much lower electrical resistivity than that of undoped graphene.

We considered two configurations of doped bi-layer graphene in our simultation (4 × 4 supercell), where the substituted (3.125%) atoms (B or N at a time) in the two layers are (a) close to and (b) far from each other. We find that configurations with dopant atoms separated by larger distance from each other are more favourable energetically. While the configuration with widely separated N atoms is lower in energy by 25 meV than the one with N at nearest sites in two planes, this energy difference for B-substitution is rather small (4 meV). This implies that homogenous B-substitution may be easier than N-substitution. The origin of this difference can be traced to the structure: B-C bond is about 0.5% longer than the C-C bond while N-C bond is about the same as C-C bond in length, resulting in significant relaxation of the structure of B-doped bilayer dominating its energetics. The interplaner separation reduces by almost 2.7% in B doped bilayer graphene while it remains almost unchanged in N-doped bilayers. We estimate the energy of formation of doped graphene from graphene and dopant atoms in the gaseous form to be 5.6 and 8.0 ev/atom for B and N doping respectively, suggesting that synthesis of B and N doped graphene should be quite possible.

Our calculations reveal that the linearity in the dispersion of the electronic bands within 1eV of the Fermi-energy is almost unchanged with B and N doping Fig. 5. Fermi-energy which is at the apex of the conical band structure near the K point of Brillouin zone of graphene, is shifted by – 0.65 eV and 0.59 eV in the case of 2 at % B and N substitutions. These shifts are of -1.0 and 0.9 eV in 3.125 at % B and N doped bilayers respectively. This results in p type semi conducting behaviour of graphene Fig. 5, as expected. We note that much (96%) of the shift in Fermi energy arises essentially from the substitution with dopants, and the remaining 4% arises from the lattice relaxation. This is also reflected in the almost symmetric shift in Fermi energy with B and N substitution, which were seen to be associated

with large and small structural relaxation respectively. It is indeed encouraging because this means that effects of doping should scale reasonably well to lower concentrations.

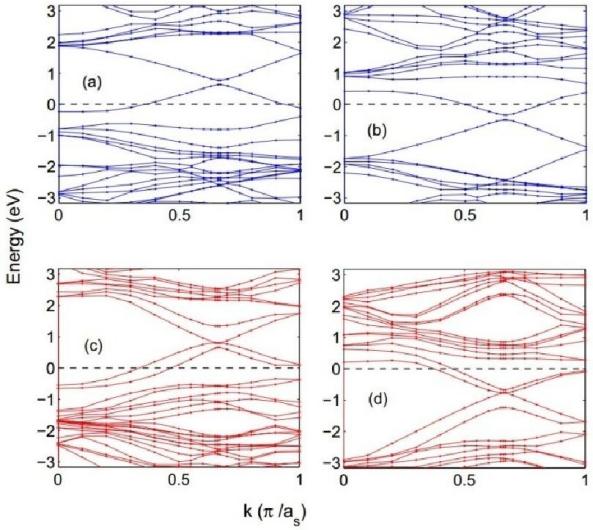

Fig. 5. Electronic structure of substitutionally doped graphene monolayer (a) and (b), and bilyaers (c) and (d), with boron and nitrogen respectively, a_s is the in-plane lattice constant of the supercell.

Table I : Various contributions to the shifts in phonon frequencies of graphene and bilayers resulting from B or N substitution.

G-band	Fixed lattice	Relaxed lattice	With dynamic correction
Pristine monolayer	1570.7	1570.7	1570.7
2% Boron doped monolayer	1579.4	1561.2	1584.6
2% nitrogen doped monolayer	1546.5	1553.4	1574.4
Pristine bilayer graphene	1603.8	1603.8	1603.8
3.125% boron nitrogen diped bilayer	1609.7	1582.4	1617.8
3.125% nitrogen doped bilayer	1566.1	1577.7	1609.9
D-bands	Frequency (cm^{-1})	D-band shift (cm^{-1})	2D-band shift (cm^{-1})
Pristine bilayer graphene	1404.1	0.0	0.0
3.125% boron doped bilayer	1387.2	–16.9	– 33.2
3.125% nitrogen doped bilayer	1400.0	– 4.1	– 8.2

Raman spectroscopy is ideally suited for the characterization of doped graphene [6-11]. It is important to know how it correlates with the concentration of carriers or dopants. The shift in the G band frequency measured by Raman Spectroscopy has many physical contributions and we use our calculations to uncover the relative magnitudes of these [12, 16]. Unexpected purely on the basis of the lengths of B-C and N-C bonds, in the context of carbon nano-tubes, Yang and Coville [17-19] had reported an interesting findings that the G band shifts are in the same direction. Very similar changes in the G band of bilayer graphene Table I are estimated from our calculations with B and N substitution, assuming the same amount of dynamic corrections as in the mono-layer. This assumption is reasonable for shifts in Fermi energy above 0.39 eV and less than 1 eV (the second band is populated by electrons or holes, as seen Fig. 4, because the density of states of the bilayer matches with that of the monolayer and hence the dynamic corrections are expected to be similar Figs. 4 and 5.

Thus, the comparison between experiment and calculations shown here can be used to conclude that dynamic corrections are important in understanding the changes in the phonon frequencies of graphene and of bilayers arising from the introduction of carriers. In fact, the overall neutrality of substitutionally doped graphene allows a very clean and accurate calculation and further testing of the role of dynamic corrections arising from doping to the G band in graphene [20-25].

Our observation on the non-segregating tendency or the homogeneity in the distribution of boron implies that the disorder or the number of possible configurations will increase with the concentration of dopant atoms and result in more prominent peaks of the D-band, as evidenced in the measured Raman spectra reported here Fig. 4. Secondly, the changes in frequency of the Raman 2D band can be understood from our results for the phonons at $K + \Delta K$ accessible in the spectrum of Γ point phonons, determined for the 4 × 4 supercell. We find that the shifts in the frequency of phonons at $K + \Delta K$ are comparable to the observed values Table I, and much weaker in magnitude than the ones at *K,* reaffirming the strong Kohn-anomaly in the phonons at the K point. We note that the eigen modes of the G band and D band Fig. 6 also change with doping by developing features in the atomic displacements localized near the dopant atoms, providing a physical picture why these modes could be used to characterize the nature of dopant atom and its effects on the electronic structure of graphene or of bilayer graphene [26-27].

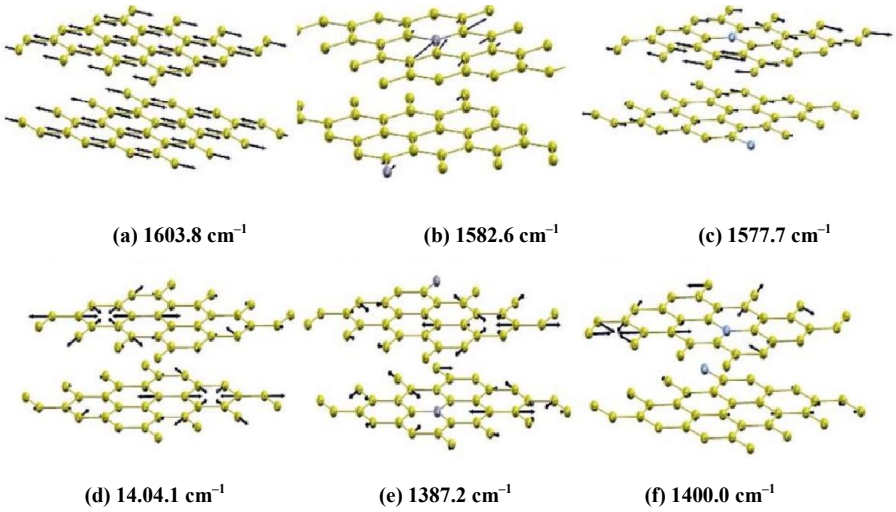

(a) 1603.8 cm^{-1} **(b) 1582.6 cm^{-1}** **(c) 1577.7 cm^{-1}**

(d) 14.04.1 cm^{-1} **(e) 1387.2 cm^{-1}** **(f) 1400.0 cm^{-1}**

Fig. 6. Atomic displacements of the G-band and D-band modes calculated (a) and (d) for pristine bilayers, (b) and (e) for B doped bilayers, and (c) and (f) for N-doped bilayers.

Sample characterization : By X-ray diffraction (XRD) method of the samples were recorded in the $\theta - 2\theta$ Bragg-Bretano geometry with a siemens D5005 diffractometer using Cu $K_\alpha \left(\lambda = 0.15148\,\text{nm}\right)$ radiation. Raman spectra were recorded with LabRAM HR high resolution Raman spectrometer (Horiba Jobin Yvon) using He-Ne Laser $\left(\lambda = 632.8\,\text{nm}\right)$. Transmission electron microscope (TEM) images were obtained with a JEOL JEM 3010 instrument. Atomic force microscope (AFM) measurements were performed using NanoMan. X-ray photoelectron spectroscopy (XPS) was recorded using a VG scientific ESCA LAB V spectrometer. EELS were recorded with a transmission electron microscope (FEI,

TECHAIF30) equiped with an energy filter for EELS operating at 200kV. Thermogravimetric analysis was carried out using Mettler Toledo TGA 850 instrument.

Conclusion

We used ab-intio density functional theory to investigate the effect of the B and N doped graphene. XPS signals of B and N doped graphene, TEM images, calculated scanning tunneling microscopy and Raman spectra of undoped graphene samples, electron structure of doped graphene monolayer and bilayers. Atomic displacements of the G band and D band mode calculated. Finally our results are useful to provide an explanation of the B5 H6 diborane structure. A further study should be performed to shed light on this issue, in particular energy path and activation barrier.

Acknowledgement

The authors are thankful to Prof. Jai Shankar, Department of Physics, Institute of Basic Science, Khandari Campus, Dr. B.R. Ambekdar University, Agra, for his valuable suggestions in synthesis and characterization of samples in the present work.

References

1. Hill, E.W., Geim, A.K., Novoselov, K., Schedin, Blake, P.F., Graphene spin valve devices. *IEEE Trans. Mang.* **42**, 2694-2696 (2006).
2. Geim, A.K. and Novoselov, K.S., *Nature Mater*, **6**, 183 (2007).
3. Katsnelson, M.I., *Materials Today,* **10**, 20 (2007).
4. Novoselov, K.S., Jiang, Z., Zhang, Y., Morozov, S.V., Stormer, H.L., Zeitler, U., Maan, J.C., Boebinger, G.S., Kim, P. and Geim, K., *Science,* **315**, 1379 (2007).
5. Novoselov, K.S., Geim, A.K., Morozov, S.V., Jiang, D., Zhang, Y., Dubonos, S.V., Grigorieva, I.V. and Firzov, A.A., *Science,* **306**, 666 (2004).
6. Das, A., Pisana, S., Chakraborty, B., Piscanec, S., Saha, S.K., Waghmare, U.V., Novoselov, K.S., Krishnamurthy, H.R., Geim, A.K., Ferrari, A.C. and Sood, A.K., *Nature Nanotech*., **3**, 210 (2008).
7. Das, B., Voggu, R., Rout, C.S. and Rao, C.N.R., *Chem. Comm*., 5155 (2008).
8. Voggu, R., Das, B., Rout, C.S. and Rao, C.N.R., *J. Phys.: Condens. Matter,* **20**, 472204 (2008).
9. Ferrai, A.C., Meyer, J.C., Scardaci, V., Casiraghi, C., Lazzeri, M., Mauri, F., Piscanec, S., Jiang, D., Novoselov, K.S., Roth, S. and Geim, A.K., *Phys. Rev. Lett*., **97**, 187401 (2006).
10. Ferrai, A.C., *Solid State Commun.,* **143**, 47 (2007).
11. Subrahmanyam, K.S., Vivekchand, S.R.C., Govindaraj, A. and Rao, C.N.R., *J. Matert. Chem.,* **13**, 1517 (2008).
12. Ohta, T., Bostwick, A., Seyller, T., Horn, K. and Rotenberg, E., *Science,* **313**, 951 (2006).
13. Panchakarla, L.S., Govindraj, A. and Rao, C.N.R., *ACS Nano,* **1**, 494 (2007).
14. Sen, R., Satishkumar, B.C., Govindaraj, A., Harikumar, K.R., Raina, G., Zhand, J.P., Cheetham, A.K. and Rao, C.N.R., *Phys. Lett.,* **287**, 671 (1998).
15. Dresselhaus, M.S. and Eklund, P.C., *Advances in Physics,* **49**, 705 (2000).
16. Cancado, L.G., Takai, K., Enoki, T., Endo, M., Kim, Y.A., Mizusaki, H., Jorio, A., Coelho, L.N., Paniago, R.M. and Pimenta, M.A., *Appl. Phys. Lett*., **88**, 163106 (2006).
17. Yang, Q., Hou, P., Unno, M., Yamauchi, S., Saito, R. and Kyotani, T., *Nano Lett*., **5**, 2465 (2005).
18. Mandal, K.C., Strydom, A.M., Erasmus, R.M., Keartland, J.M., Coville, N.J., *Mater. Chem. Phys*., **111**, 386 (2008).
19. Nxumalo, E.N., Nyamori, V.O. and Coville, N.J., *J. Organomet. Chem.,* **692**, 2942 (2008).
20. Ando, T., *J. Phys. Soc. Jpn.,* **75**, 124701 (2006).
21. Lazzeri, M. and Mauri, F., *Phys. Rev. Lett.,* **97**, 266407 (2006).
22. Ando, T., *J. Phys. Soc. Jpn.,* **76**, 104711 (2007).
23. Baroni, S., deGironcoli, S., Dal, Corso A., Giannozzi, P., http://www.pwscf.org.

24. Perdew, J.P., Burke, J. and Ernzerhof, M., *Phys. Rev. Lett.,* **77**, 3865 (1996).
25. Perdew, J.P. and Zunger, A., *Phys. Rev. B,* **23**, 5048 (1981).
26. Saha, S.K., Waghmare, U.V., Krishnamurthy, H.R. and Sood, A.K., *Phys. Rev. B,* **76**, 201404 (2007).
27. Saha, S.K., Waghmare, U.V., Krishanamurthy, H.R. and Sood, A.K., *Phys. Rev. B*, **78**, 165421 (2008).

❑